Stages of Infection during the Tripartite Interaction between *Xenorhabdus nematophila*, Its Nematode Vector, and Insect Hosts

Mathieu Sicard,[1] Karine Brugirard-Ricaud,[2] Sylvie Pagès,[2] Anne Lanois,[2]
Noel E. Boemare,[2] Michel Brehélin,[2]* and Alain Givaudan[2]*

*Laboratoire GPIA, Université Montpellier II-CNRS-IFREMER (UMR5171),[1] and Laboratoire EMIP,
Université Montpellier II, IFR 122, Institut National de la Recherche Agronomique
(UMR1133),[2] Montpellier, France*

Bacteria of the genus *Xenorhabdus* are mutually associated with entomopathogenic nematodes of the genus *Steinernema* and are pathogenic to a broad spectrum of insects. The nematodes act as vectors, transmitting the bacteria to insect larvae, which die within a few days of infection. We characterized the early stages of bacterial infection in the insects by constructing a constitutive green fluorescent protein (GFP)-labeled *Xenorhabdus nematophila* strain. We injected the GFP-labeled bacteria into insects and monitored infection. We found that the bacteria had an extracellular life cycle in the hemolymph and rapidly colonized the anterior midgut region in *Spodoptera littoralis* larvae. Electron microscopy showed that the bacteria occupied the extracellular matrix of connective tissues within the muscle layers of the *Spodoptera* midgut. We confirmed the existence of such a specific infection site in the natural route of infection by infesting *Spodoptera littoralis* larvae with nematodes harboring GFP-labeled *Xenorhabdus*. When the infective juvenile (IJ) nematodes reached the insect gut, the bacterial cells were rapidly released from the intestinal vesicle into the nematode intestine. *Xenorhabdus* began to escape from the anus of the nematodes when IJs were wedged in the insect intestinal wall toward the insect hemolymph. Following their release into the insect hemocoel, GFP-labeled bacteria were found only in the anterior midgut region and hemolymph of *Spodoptera* larvae. Comparative infection assays conducted with another insect, *Locusta migratoria*, also showed early bacterial colonization of connective tissues. This work shows that the extracellular matrix acts as a particular colonization site for *X. nematophila* within insects.

Bacteria of the genus *Xenorhabdus* (*Enterobacteriaceae*) are mutually associated with entomopathogenic nematodes of the genus *Steinernema* (25). These bacteria, which are highly pathogenic to insects, are transported by their nematode vectors into the hemocoel of the insect host, which then dies, probably due to a combination of the effects of toxins and septicemia. The bacteria contribute to the mutualistic relationship by establishing and maintaining suitable conditions for nematode reproduction in the insect cadaver (23). Among the newly produced nematodes, the infective juveniles (IJs) reassociate with the mutualistic bacteria before leaving the insect cadaver (14). IJs transport *Xenorhabdus* cells in a special organ within the intestine known as the "vesicle of Bird and Akhurst" (2). Martens et al. (14) recently showed that the IJs undergo predominantly monoclonal colonization and that the bacteria also multiply within the vesicle.

Possible routes of insect infection by bacterium-helminth complexes include the alimentary tract, via the anus and mouth. Direct penetration of the insect cuticle by *Steinernema* has never been described, but nematodes may enter the body cavity via the tracheal system if the aeropyles of the spiracles are wider than the diameter of the IJs (9, 20). Few studies have described subsequent steps in insect body colonization by the two partners. Poinar and Himsworth (18) reported that IJs within the midgut of the greater wax moth, *Galleria mellonella*, shed their old cuticle, and penetrated the hemocoel via the midgut wall. Once in the hemocoel, *Xenorhabdus* has been found to be released into the hemolymph from IJs. However, the signals triggering the shedding of the cuticle and bacterial release remain unknown.

Nothing is known about bacterial colonization of the insect tissues or organs following the arrival of the bacterium in the insect hemocoel. In vivo and in vitro studies have tended to focus on the interaction between the *Steinernema carpocapsae-Xenorhabdus nematophila* complex and the insect immune system (for a review, see reference 7). Various studies have shown that the nematobacterial complex attenuates insect cellular reactions in the hemolymph. The inhibition of nodule formation was studied in vivo (8, 16, 17), and cytotoxic factors active against hemocytes have been identified in vitro (4, 21, 22). The mode of action of a cytolytic factor on immunocytes (cells of the insect hemolymph) was recently characterized in detail (22).

We investigated the early steps of insect colonization by the bacterial symbiont by constructing a green fluorescent protein (GFP)-labeled *X. nematophila* strain. This made it possible to visualize directly, by microscopy, bacteria in living nematodes and within insect tissues after artificial infection by injection or after natural nematode infestations. For both routes of infec-

tion, we found that living *Xenorhabdus* cells had an extracellular life cycle and initially occupied two specific sites in the insect: the hemolymph plasma and connective tissues of the anterior midgut in the lepidopteran *Spodoptera littoralis*. We investigated whether this specific site was related to the presence of connective tissues or the insect midgut by carrying out comparative infection experiments with another insect, the orthopteran *Locusta migratoria*.

MATERIALS AND METHODS

GFP labeling of *X. nematophila*. *X. nematophila* was labeled with GFP by conjugation with pBBR1-KGFP (15) containing a constitutive promoter randomly incorporated upstream from the *gfpmut3* gene. An *X. nematophila* promoter library was constructed by digesting chromosomal DNA with Sau3A. Fragments of 0.2 to 1.5 kb in size were ligated into the single BamHI site immediately upstream from the *gfpmut3* gene in pBBR1-KGFP. The ligation mixture was introduced into *Escherichia coli* DH5α by transformation, and 160 kanamycin-resistant colonies were screened for constitutive promoter activity by means of epifluorescence microscopy (Leica). Five recombinant plasmids from GFP-positive clones were used to transform *E. coli* S17.1 and were subsequently introduced into *X. nematophila* F1 by mating. Three kanamycin-resistant exconjugants from each mating were assessed, and clone D3, with the highest level of fluorescence, was analyzed further. We compared the F1D3 clone with the wild type by phenotypic characterization, as previously described (10), and found no difference between the two strains. F1D3 also displayed bright, stable fluorescence on nonselective media.

Production of *Steinernema carpocapsae* (strain Plougastel)-*X. nematophila* (F1D3) associations. *Steinernema carpocapsae* (strain Plougastel) naturally associated with *X. nematophila* (strain F1) was maintained by passage through larval-stage *G. mellonella* and harvested on White traps (27). Surface-sterilized eggs were obtained by crushing 40 mature nematode females in sterile Ringer's solution (Aguettant, Lyon, France) supplemented with sodium hypochlorite (10%, wt/vol) for 18 min. The disinfected eggs were transferred to liver-agar plates (15 g of biotrypticase [Difco] per liter, 5 g of biosoyase [Difco] per liter, 5 g of NaCl per liter, 15 g of agar [Difco] per liter, 2 g of brewer's yeast per liter, 100 g of calf liver per liter) and incubated at 24°C for 3 weeks, after which axenic IJs were obtained. Sterility was assessed by inoculating nutrient broth tubes with nematode samples from the liver-agar plates. Axenic IJs were harvested from liver-agar plates as previously described (26). Monoxenic cultures of *Steinernema carpocapsae* were obtained by incubating 1,000 axenic IJs with 100 μl of overnight culture of *X. nematophila* strain F1D3 or *X. nematophila* strain F1. We monitored the growth of the nematode culture and, after 3 weeks, collected IJs in sterile Ringer's solution, as previously described (26). Freshly harvested IJs and IJs incubated in Ringer's solution at 28°C for 90 and 180 days were observed by epifluorescence microscopy to determine the number of nematodes that retained GFP-labeled *X. nematophila*.

In vitro release of bacteria from nematodes. The release of *X. nematophila* from IJs was observed by mixing a 10-μl sample containing 50 IJs with an equal volume of test material (hemolymph and gut contents) in an Eppendorf tube. The mixture was incubated for 2 h at room temperature, and IJs were then deposited between the slide and coverslip and viewed with an epifluorescence microscope. Insect hemolymph was collected by bleeding fourth-instar larvae of *Spodoptera littoralis*. This was achieved by making a lesion in a proleg. The gut of *Spodoptera littoralis* was dissected, and its contents were collected. Briefly, each larva was anesthetized (incubation for 3 min below 0°C) and its cuticle was dissected dorsally. The gut was then ligatured at each end, removed from the body of the insect, and thoroughly rinsed in phosphate-buffered saline. The gut wall was opened and the midgut content, wrapped in the peritrophic matrix, was collected and observed by phase-contrast and epifluorescence microscopy. The release of bacteria from individual nematodes was investigated after 2 h of contact between the insect fluids and the IJs.

Insect infections. The common cutworm, *Spodoptera littoralis*, and the locust, *L. migratoria*, were reared on an artificial diet at 23°C (19) and on grass at 30°C, respectively, with a photoperiod of 12 h. Fifth-instar larvae were used.

(i) Infection with GFP-labeled bacteria. Experiments were performed as previously described (10). Briefly, the surfaces of insect larvae were sterilized with 70% (vol/vol) ethanol. A Hamilton syringe was then used to inject groups of 20 larvae with 20 μl each of the appropriate dilution in phosphate-buffered saline of 20-h cultures containing low (400 to 800 bacteria) and high (about 10^4 bacteria) doses of the GFP-labeled strain F1D3 or the wild-type strain F1, depending on

the experiments. Treated larvae were incubated individually for up to 96 h, and the times of death of the insects were recorded. Three independent experiments were performed for each treatment (bacterial strains or doses). Statistical analysis was carried out with the Statistical Package for Social Science version 11.0.1 (SPSS, Inc., Chicago, Ill.) to compare individual survival times in each group with individual survival times in the other groups.

(ii) Infestation of insect larvae with nematodes harboring GFP-labeled *X. nematophila*. Forty IJs containing GFP-labeled bacteria were counted and placed on filter paper in Eppendorf tubes, into which *Spodoptera* or *Locusta* larvae were then introduced. After 2 h of contact between nematodes and insects, insect larvae were rinsed with sterile water to prevent new infestations. All experiments were performed at 28°C and completed within 22 h of infestation.

Quantification of *X. nematophila* organisms colonizing *Spodoptera littoralis*. We counted the number of bacteria recoverable from the hemolymph following the injection of bacteria by bleeding three insect larvae per time point to collect total hemolymph fluid. We then plated serial dilutions of hemolymph in Luria broth on NBTA (nutrient agar supplemented with 25 mg of bromothymol blue per liter and 40 mg of triphenyltetrazolium chloride per liter) supplemented with erythromycin (final concentration of 15 μg/ml). Use of this medium prevents the growth of insect-associated bacteria other than *X. nematophila* F1, which is naturally resistant to erythromycin. Plates were incubated for 48 h at 28°C, and CFU were counted. Total hemolymph volume per insect larva was estimated to be about 500 μl. Results are expressed as numbers of CFU per insect (equivalent to 500 μl of hemolymph).

As it was not possible to differentiate between free and nematode-associated bacteria by counting the number of CFU in nematode infestation experiments, the number of bacterial cells in hemolymph samples was estimated using a Thoma-type counting chamber under an epifluorescence microscope.

Insect dissection, histology and electron microscopy. Insects were anesthetized by cooling and submerging them in phosphate-buffered saline (Biochrom), and pieces of various tissues and organs (muscle, midgut, trachea, ventral nervous cord, Malpighian tubules, and genital tract for *Spodoptera littoralis* and *L. migratoria* and hematopoietic tissue for *L. migratoria*) were cut off. Three pieces of about 1 mm³ from each tissue were squashed between the slide and the coverslip and observed by epifluorescence microscopy. Pieces of these organs were also fixed in 5% glutaraldehyde in 0.1 M phosphate buffer (pH 7.2), postfixed in 1% osmium tetroxide solution in the same buffer, dehydrated in alcohol, and embedded in Epon. For light microscopy, semithin sections were stained with toluidine blue. For electron microscopy, ultrathin sections were contrast stained with uranyl acetate and lead citrate and observed at 70 kV.

RESULTS

Growth of injected GFP-labeled *Xenorhabdus* bacteria in *Spodoptera* hemolymph. We assessed bacterial growth in the body of the insect by injecting precise doses of bacteria directly into the insects. Living cells of wild-type *X. nematophila* are known to be highly virulent when injected into insects (10). We compared the virulence of the GFP-labeled strain F1D3 with that the wild-type strain F1 by injecting low (400 to 800 bacteria) and high (about 10^4 bacteria) doses of the two strains into the hemocoels of *Spodoptera littoralis* larvae. When larval mortality was monitored over a 3-day-period after injection (data not shown), no significant difference ($P = 0.3$) in insect mortality was recorded between wild-type and GFP-labeled bacteria, regardless of the dose injected.

Insects began to die (up to 10% mortality) 26 h after injection for the lowest dose and 23 h after injection for the highest dose (Fig. 1). We then assessed the growth rates of F1D3 in hemolymph by measuring the number of CFU. Bacterial growth in hemolymph depended on the dose injected. Partial (2 orders of magnitude) clearance of circulating bacteria was observed during the first 3 h of exposure after the injection of low doses (Fig. 1A), but no decrease in the number of bacteria was detected in the first few hours after the injection of high doses of bacteria (Fig. 1B). As previously reported (8), 8 to 10 h after injection, the number of bacteria exceeded the in-
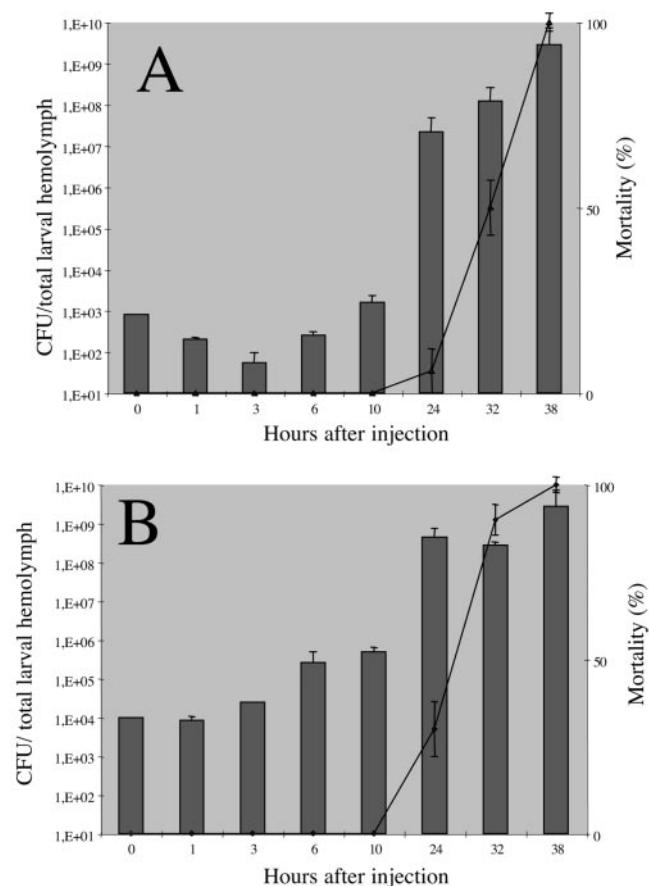
FIG. 1. Bacterial growth and insect larval mortality following the injection of *X. nematophilus* F1D3 into *Spodoptera littoralis*. The histogram shows the mean numbers of CFU recovered from the total hemolymph of single larvae (four larvae per time point). Larvae were each injected with 800 (A) and 10^4 (B) bacteria at time zero. Errors bars indicate standard errors of the means. The lines indicate mortality rates of larvae (a total of 20 larvae for each treatment) injected with 800 (A) and 10^4 (B) bacteria at time zero. Results expressed as percentages represent the averages of mortality values from three independent experiments with similar bacterial doses. Errors bars indicate standard deviations.

oculum level, demonstrating that bacterial multiplication had occurred. Septicemia also occurred before the insects died (Fig. 1). Epifluorescence microscopy observations over time showed an absence of fluorescent bacteria within or in contact with hemocytes and in hemocyte microaggregations (Fig. 2A and B). In the hemolymph, nodule formation is one of the main cellular immune reactions against bacteria. Nevertheless, only 0.34 melanized nodule per insect was observed after the injection of high doses of bacteria and no GFP-labeled bacteria were detected within these nodules.

Colonization of *Spodoptera* tissues by GFP-labeled *Xenorhabdus* cells. To detect GFP-labeled *Xenorhabdus* in sites other than the hemolymph, various *Spodoptera littoralis* larval tissues were observed by epifluorescence microscopy at various times after the injection of low doses of bacteria. All examinations were performed before the death of the insect. No bacteria were detected in the first 22 h after injection. Bacterial aggregates were detected 23 h after injection but only in the anterior

region of the midgut (Fig. 2C, D, E, and F). Bacterial aggregates were present among muscle fibers (Fig. 2C and D) and tracheae around the gut (Fig. 2E and F). All the other organs observed were free of fluorescent bacteria.

We determined the precise location of bacteria within tissues by examining anterior midgut sections of infected larvae by light microscopy (Fig. 3A). The midgut epithelium is surrounded by circular (inner) and longitudinal (outer) muscles wrapped in connective extracellular matrix and tracheae. Single bacteria and bacterial aggregates were clearly found within the connective tissue alongside the muscle bundles of the two muscular layers. This location was confirmed by transmission electron microscopy (Fig. 3C). In particular, bacteria were never observed in contact with cells of the digestive epithelium and rarely in contact with the basal lamina lining this epithelium on the hemocoel side. Bacterial aggregates were observed in contact with the extracellular laminae of the connective tissues enclosing the muscle layers and binding the bundles of fibers.

***Xenorhabdus* also colonizes connective tissue in *Locusta*.** To confirm this specific location of bacterial cells, comparative studies were carried out with another insect species, *L. migratoria* (Orthoptera). We chose to study this insect because connective tissue is more developed in orthopterans than in insects of other orders (1). Following the injection of low doses of bacteria, GFP-labeled *Xenorhabdus* was never observed in the vicinity of the locust midgut. However, as soon as 8 h after injection, bacteria were observed, but only within the hematopoietic organ (HO) (data not shown). This organ, described by Hoffmann in 1970 (12), is the site of circulating hemocyte production. By 24 to 26 h after the infection of *L. migratoria*, numerous fluorescent bacteria were observed, but only in two locations: the HO and the hemolymph, which displayed septicemia. By light microscopy (Fig. 3B) and transmission electron microscopy (Fig. 3D), the HO displayed irregular aggregate tissues consisting of reticular cells (HO-resident macrophages) and hemocytes surrounded by a thick extracellular matrix. Bacteria were observed in this connective matrix, mainly outside HO cells. Less than 10% of the bacteria were found to be present within cells, and most of these intracellular bacteria appeared to be undergoing digestion in secondary lysosomes of the reticular cells (data not shown). No nodule formation was observed in the HO or in other organs right up to the death of the insect (36 to 40 h after injection).

Colonization of IJ nematodes by GFP-labeled *X. nematophila*. We monitored colonization of insects by *X. nematophila* following *Steinernema carpocapsae* infestation by producing infective juveniles harboring GFP-labeled *Xenorhabdus*. The time at which the first gravid females appeared and the colonization of liver-agar plates by nematodes were identical following coculture on lawns of the wild-type strain F1 and the GFP-labeled strain F1D3. Epifluorescence microscopy of IJs clearly showed that GFP-labeled *X. nematophila* organisms were located within the vesicle in the anterior ventricular portion of the IJ intestine (Fig. 4A and B), as previously described for other species of *Steinernema* (2). Counts performed under an epifluorescence microscope showed that 96% of freshly harvested IJ nematodes had vesicles containing fluorescent bacteria. The survival rate for IJs was 80% after incubation for 90 days in Ringer's solution at 24°C. A vesicle containing
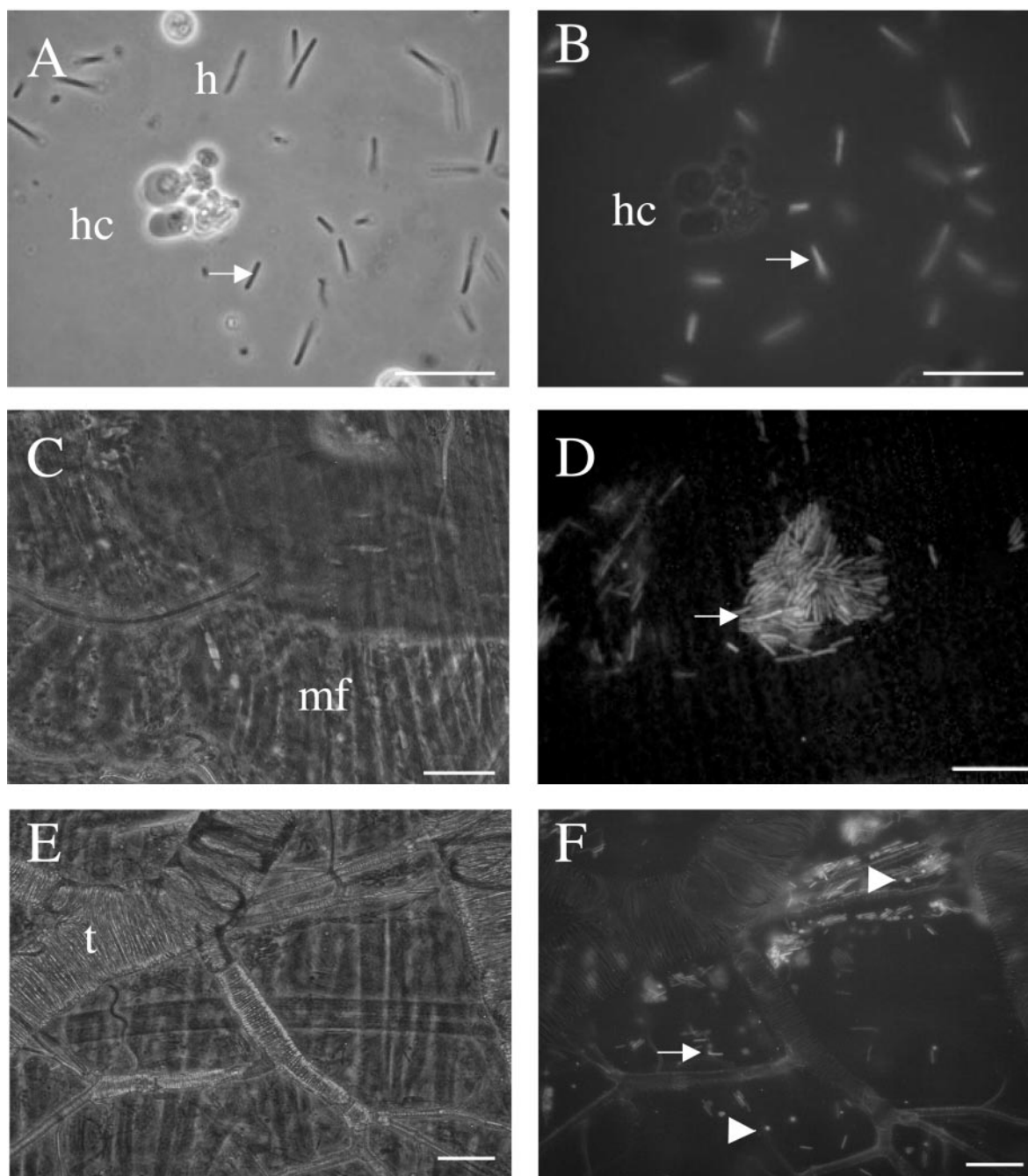
FIG. 2. Detection of GFP-labeled *Xenorhabdus* in *Spodoptera littoralis* tissues 23 h after injection. The same field views are presented in phase contrast (left) and with epifluorescence (right). (A, B) Free bacteria within the insect hemolymph. Note that no bacteria were seen within hemocytes (h) or surrounded by hemocyte aggregate (hc). (C to F) Pieces of the anterior region of the midgut were squashed and observed. Single bacteria and aggregates were detected under muscle fibers (mf) (C and D) and alongside trachea (t) (E and F). Note that numerous fluorescent rounded cells (arrowhead) were observed at this site (F). Arrows show bacteria. Bars represent 10 μm.

GFP-labeled bacteria was detected in 96% of these aged IJs. In contrast, bacteria were observed at various locations outside the vesicle in dead IJs (Fig. 4C). After 180 days of incubation, all nematodes were dead and for all of those carrying GFP-labeled bacteria, the bacteria were located outside the vesicle.

In vitro release of bacteria from nematodes. Before infesting insects with GFP-labeled *Xenorhabdus* IJ complexes, we inves-

tigated bacterial release in vitro. No living nematodes taken from liver-agar plates released their bacteria during epifluorescence microscopy observations. If IJs were incubated for 2 h in collected insect fluids, such as hemolymph and gut contents, 46 and 90% of nematodes, respectively, lost their second cuticle. In contact with hemolymph, 27% of the IJs had GFP-labeled bacterial aggregates in the anterior part of the intesti-
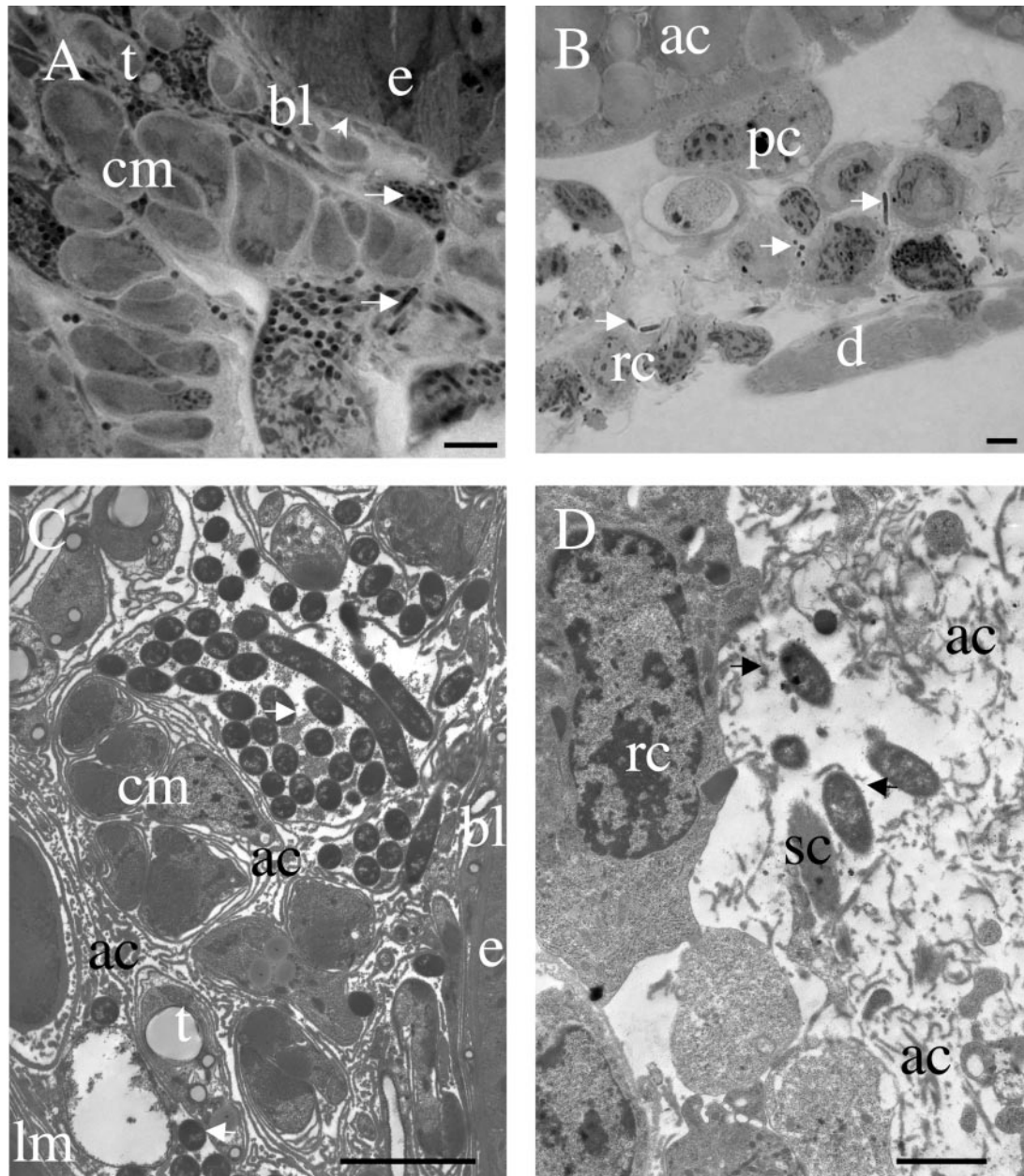
FIG. 3. Details of connective tissue colonization by *X. nematophila*. (A) Light micrograph of a toluidine blue-stained semithin section of *Spodoptera littoralis* midgut wall, 23 h after the injection of low doses of *X. nematophila* F1D3. Note that single bacteria and bacterial aggregates (arrows) are dispersed among tracheae (t) and bundles of myofibrils of circular muscles (cm), often far from the basal lamina (bl) of the digestive epithelium (e). (B) Light micrograph of a toluidine blue-stained semithin section of the HO from *L. migratoria* 26 h after the injection of 400 *X. nematophila* F1D3 organisms. Single bacteria are observed among reticular cells (rc), between the muscles of the dorsal diaphragm (d), in pericardial cells (pc), and in adipose cells (ac). (C) Transmission electron micrograph of *Spodoptera littoralis* midgut wall (same conditions as described for panel A). Note the extracellular location of bacteria among the highly developed amorphous fibers of connective tissue (ac) between the digestive epithelium (e), circular muscles (cm), longitudinal muscles (lm), and tracheae (t). (D) Transmission electron micrograph of a locust HO (same conditions as described for panel B). Bacteria are observed outside the macrophagic reticular cells (rc) and between amorphous (ac) and structured (sc) fibers of connective tissue. Bars represent 2 μm in panels A, B, and D and 5 μm in panel C.

nal lumen, 63% had a bacterial aggregate with additional fluorescent single bacteria circulating throughout the intestinal lumen, whereas only 10% had residual ventricular vesicles. If bacteria were released from IJs that had not begun to shed the second cuticle, GFP-labeled bacteria were observed between the two cuticles (data not shown). In contact with the contents of the insect gut, all exsheathed juveniles had brightly fluorescent bacteria within their ventricular vesicles and no fluorescent bacteria migrated throughout the nematode intestine towards the anus.

Colonization of insects by IJ nematode-GFP-labeled bacterial complexes. We characterized the early stages of insect
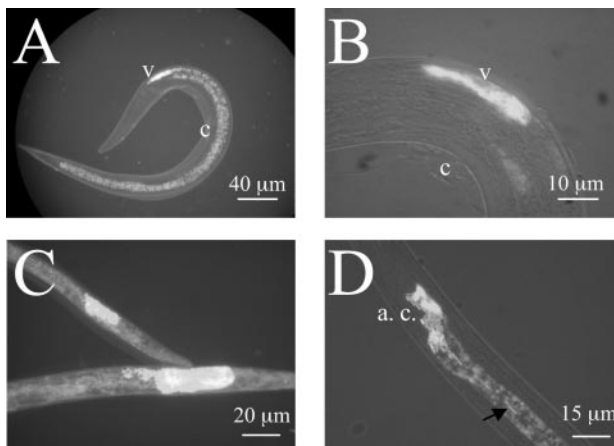
FIG. 4. Location of GFP-labeled *X. nematophila* cells in the intestines of *Steinernema carpocapsae* IJs. (A and B) *X. nematophila* cells located in the vesicle (v) of the IJs protected by the cuticle of the second larval stage (c). (C) The IJs that died after incubation in Ringer's solution at 24°C for 90 days showed fluorescent bacteria that grew in locations other than the vesicle. (D) Release of GFP-labeled *X. nematophila* by IJ nematodes collected from the guts of *Spodoptera* larvae: bacterial cells (arrow) leaving the aggregate (a. c.) of bacteria in the anterior part of the IJ and migrating through the IJ intestine toward the anus.

colonization in vivo by infecting fifth-instar larvae of *Spodoptera littoralis* with IJ-GFP-labeled bacterial complexes. During the first stage of infestation (3 to 5 h), 16 insects underwent hemolymph sampling and dissection. No fluorescent bacteria were observed in insect hemolymph 5 h after nematode entry, and IJs were found only in the guts of the insects. All of these IJs were exsheathed in the insect midgut. At this time, 14% had brightly fluorescent ventricular vesicles; 20% had GFP-labeled bacterial aggregate in an axial position, probably related to the beginning of the bacterial release process. We found that 28% of IJs showed both features: a bacterial aggregate in an axial position and fluorescent bacteria spreading throughout the nematode intestine (Fig. 4D). In this case, bacteria were observed to migrate by pulses, through the posterior region of the intestine towards the anus. Finally, 38% of IJs were completely cleared, and these nematodes were mostly wedged into the midgut wall and in the lumen of Malpighian tubules. From 5 to 14 h after infestation, we sampled two insects every 2 h. The number of bacteria per insect increased from 6×10^6 to 3×10^8 during this phase. Following the dissection of insects and direct examination under the epifluorescence microscope, we observed the appearance of GFP-labeled aggregates in the anterior region of the midgut only, 12 to 14 h after infestation (data not shown), as was observed following bacterial injection (see above). The first larval deaths were recorded 16 h after infestation, and after 20 h, all *Spodoptera* larvae were dead.

We carried out IJ infestations of *Locusta* larvae to validate the HO as a specific site of infection in Orthoptera following the release of bacteria from the nematode. Soon after infestation (3 to 5 h), fluorescent bacterial cells were observed dispersed in the HO and hemolymph, whereas no bacteria were seen in the other tissues. At 20 h after infestation, large bacterial aggregates appeared in the HO (data not shown), demonstrating active growth at this site, whereas only dispersed

bacteria were seen at other locations. The *Locusta* larvae were all dead 22 h after infection.

DISCUSSION

Previous studies have described the life cycle of *Xenorhabdus* in its nematode host (14) or in the hemolymph of insect larvae (8). However, colonization of the body of the insect by *Xenorhabdus* following its release from the nematode, right through to the development of septicemia in the insect hemolymph, had not been described. In particular, little is known about the process of bacterial infection in the insect and the sites colonized by *Xenorhabdus*. Constitutive promoters for GFP production provide a useful tagging system for bacteria. In this study, we showed that the tagging of *X. nematophila* with *gfp* did not impede virulence in insects or their mutualistic association with nematodes in comparison with the wild-type strain. The labeling of *Xenorhabdus* with GFP and the ease with which insect tissues can be dissected made it possible to visualize bacteria in living nematodes and to locate the pathogen in specific insect tissues.

Various stimuli trigger the release of bacteria from nematodes. In our experiments, most (96%) of the *Steinernema carpocapsae* IJs collected after growth in vitro on GFP-labeled *X. nematophila* lawns were brightly fluorescent. In similar experiments, Ciche and Ensign (5) showed that 74% of *Heterorhabditis bacteriophora* IJs cultured on GFP-labeled *Photorhabdus luminescens* lawns contained no visible bacteria. Thus, the high level of *gfp* expression in *Photorhabdus* seems to lead to a defect of *Heterorhabditis* nematode colonization that was not observed for *Steinernema carpocapsae*-fluorescent *X. nematophila* associations.

Our findings confirm previous reports (2, 14, 18) stating that *Xenorhabdus* in living IJs is strictly restricted to the intestinal vesicle. When IJs were incubated for 3 months, the *X. nematophila* cells continued to produce GFP. This finding strongly suggests that the bacterial aggregates in each IJ are renewed by the slow multiplication of bacteria. Moreover, bacterial growth within the intestinal vesicle has already been reported to occur in the early stages of colonization (14). The dissection of *G. mellonella* larvae after contact with IJs has demonstrated that nematodes, which presumably enter via the mouth or anus, are initially found in the insect alimentary tract and Malpighian tubules, where they immediately shed their second cuticle (18). We confirmed these observations with nematode-GFP-labeled bacterial complexes and another lepidopteran, *Spodoptera littoralis*. Furthermore, our in vitro studies revealed that contact with insect gut content is more likely to trigger the exsheathing of IJs than contact with hemolymph. Moreover, GFP labeling showed that the process of bacterial release from the vesicle into the IJ intestine certainly began in the digestive tract of the insect. The first event in this process is the relocation of the bacterial aggregate from a ventricular to an axial position. The bacteria within the nematode intestine then began to migrate towards the anus once the nematodes had crossed the peritrophic matrix, and nematode clearance was observed when the nematodes managed to work their way through the gut wall in *Spodoptera*. As about a third of the IJs released their bacteria while penetrating the gut wall, a fraction of the *Xenorhabdus* population may be released into the insect alimentary tract.

However, the in vitro incubation of IJs in insect fluids showed that the bacteria were unable to leave the IJs if they were incubated with gut contents but that they were released if they were incubated with hemolymph. Recently, Ciche and Ensign (5) reported that the nematode regurgitation of *Photorhabdus* was induced by a low-molecular-weight component present in arthropod hemolymph. The passage of nematodes through the insect midgut wall probably leads to a flow of hemolymph into the ectoperitrophic matrix space during in vivo infestations, and this may account for the lack of release stimuli in gut contents collected in vitro. Thus, the visualization of *Xenorhabdus* in IJ nematodes provided new insights into the occurrence of stimuli triggering bacterial release in the insect midgut in the early stages of colonization.

***Xenorhabdus* has an extracellular lifestyle in hemolymph.** It has long been known that *X. nematophila* multiplies in insect hemolymph (8). We show here that bacterial growth in hemolymph depended on the dose of bacteria injected. Following the injection of low doses of bacteria, the partial clearance of circulating bacteria was observed during the first 3 h, and then bacteria began to increase in number 10 h after injection (Fig. 1A). The clearance of *X. nematophila* from hemolymph occurs within minutes of infection with *G. mellonella* (Lepidoptera), and it has been suggested that cellular-defense reactions are involved in the clearance of *Xenorhabdus* cells (8). The bacteria must deal with insect cellular immune reactions, such as phagocytosis and nodule formation. Nodules are cellular formations of hemocytes and melanin, in which bacteria may become entrapped. Phagocytosis and nodulation are each able to clear thousands of nonpathogenic bacterial cells from circulating hemolymph within 1 h of infection (13). It has been suggested that the reappearance of *Xenorhabdus* in the hemolymph results from the multiplication of bacteria within nodules (7). We show here that, following the injection of living *X. nematophila* cells into *Spodoptera littoralis*, very few nodules per insect were formed. In addition, no fluorescent bacteria were found adhering to or entering hemocytes from the *Spodoptera* hemolymph. This finding was confirmed by electron microscopy studies (M. Brehélin and A. Givaudan, unpublished data). It is likely that living *X. nematophila* cells promote their own extracellular life cycle in insects. During infection of insects by *Photorhabdus*, it has been shown that the bacteria persist by suppressing hemocyte-mediated phagocytosis (24). Moreover, eicosanoids, including prostaglandins and various lipoxygenase products, are thought to mediate cellular and some humeral immune responses to bacterial infection (17). It was recently shown that *X. nematophila* inhibits nodule formation by disturbing the eicosanoid pathway in *Spodoptera exigua* (16) and *Manduca sexta* (17). Overall, these data suggest that *X. nematophila* organisms have evolved mechanisms of evading the cellular innate defenses of insects by not being bound and phagocytosed by the insect hemocytes and by inhibiting hemocyte-mediated nodule formation.

The most attractive tissue for bacterial colonization is the connective tissue. Regardless of the route of infection (bacterial injection or infestation by nematobacterial complexes), GFP-labeled *X. nematophila* organisms were initially recovered from only two tissues: the connective matrix around the midgut and the hemolymph of *Spodoptera littoralis*. A recent study (24) of the colonization of *M. sexta* (lepidopteran) larvae by *P.* *luminescens*, a bacterial species closely related to *Xenorhabdus*, also suggested that the midgut and hemolymph are initially more extensively colonized than other tissues. As previously reported for *Photorhabdus* (24), tracheae are a potential route of entry of *Xenorhabdus* into the extracellular matrix (Fig. 2F) but may also provide a route for the subsequent invasion of other tissues of *Spodoptera* larvae. Nevertheless, our electron microscopy studies of *Spodoptera* infections revealed that *Xenorhabdus* cells were never observed in contact with the epithelium midgut but were instead seen within the extracellular matrix. It has been stressed that connective tissues are much more sparse in insects than in vertebrates (1). In a lepidopteran such as *Spodoptera*, a moderately developed connective tissue encloses the belts of muscle around the midgut. For orthopterans, a well-developed connective tissue, with specialized cells and extracellular material often organized into structured fibers (collagen), has been described (1). Such connective tissues are particularly well developed in the HO (12) along the dorsal vessel in *L. migratoria*. We investigated whether the attraction of the bacteria to this particular niche was due to the presence of connective tissues or to the insect midgut per se, and we carried out infection experiments with *L. migratoria*. We show here that GFP-labeled *X. nematophila* organisms were present exclusively in the hematopoietic organ and never in the vicinity of the midgut epithelium, regardless of the mode of infection, in locusts. Light and electron microscopy studies of locust organs confirmed the presence of bacteria only in the connective tissue of the HO. Sessile macrophages have been identified in the HO, which was previously described as a phagocytic organ by Cuénot (6). Bacteria of various species are regularly found in these macrophages (11). After infections with *X. nematophila*, only 10% of the bacteria were present in macrophages, with most of the bacteria being present outside the cells, among the connective fibers of the HO. Moreover, there is a lack of macrophages in the connective tissue of *Spodoptera littoralis* organisms, in which bacterial aggregates were found around the midgut. Overall, these data suggest that the connective tissue (rather than the macrophages or gut epithelium) acts as a site for bacterial colonization within the insects.

As insect hemolymph, like mammalian blood (3), may be regarded as a specialized form of connective tissue, it seems likely that *Xenorhabdus* can grow only in connective tissue during the first steps of insect colonization. Moreover, Bird and Akhurst (2) showed that the vesicles of nematode juveniles are filled with an amorphous matrix, in which *Xenorhabdus* spp. become embedded. We therefore suggest that, during its life cycle in both invertebrate hosts, *X. nematophila* initiates infection by interacting specifically with as-yet-unidentified extracellular matrix components.

REFERENCES

1. **Ashhurst, D. E.** 1985. Connective tissues, p. 249–287. *In* G. A. Kerkut and L. I. Gilbert (ed.), Comprehensive insect: physiology, biochemistry and pharmacology, vol. 3. Pergamon Press, Oxford, United Kingdom.
2. **Bird, A. F., and R. J. Akhurst.** 1983. The nature of the intestinal vesicle in nematodes of the family Steinernematidae. Int. J. Parasitol. **13:**599–606.

3. **Bloom, W., and D. W. Fawcett.** 1975. A textbook of histology. W. B. Saunders Company, Philadelphia, Pa.

4. **Brillard, J., C. Ribeiro, N. Boemare, M. Brehelin, and A. Givaudan.** 2001. Two distinct hemolytic activities in *Xenorhabdus nematophila* are active against immunocompetent insect cells. Appl. Environ. Microbiol. **67:**2515–2525.

5. **Ciche, T. A., and J. C. Ensign.** 2003. For the insect pathogen *Photorhabdus luminescens*, which end of a nematode is out? Appl. Environ. Microbiol. **69:**1890–1897.

6. **Cuénot, L.** 1896. Etudes physiologiques sur les Orthoptères. Arch. Biol. **14:**293–341.

7. **Dowds, B. C. A., and A. Peters.** 2002. Virulence mechanisms, p. 79–98. *In* R. Gaugler (ed.), Entomopathogenic nematology. CABI Publishing, Boca Raton, Fla.

8. **Dunphy, G. B., and G. S. Thurston.** 1990. Insect immunity, p. 301–323. *In* R. Gaugler and H. K. Kaya (ed.), Entomopathogenic nematodes in biological control. CRC Press, Boca Raton, Fla.

9. **Georgis, R., and N. G. M. Hague.** 1981. A neoplectanid nematode in the larch sawfly *Cephalcia lariciphila* (Hymenoptera: Pamphiliidae). Ann. Appl. Biol. **99:**171–177.

10. **Givaudan, A., and A. Lanois.** 2000. *flhDC*, the flagellar master operon of *Xenorhabdus nematophilus*: requirement for motility, lipolysis, extracellular hemolysis, and full virulence in insects. J. Bacteriol. **182:**107–115.

11. **Hoffmann, D., M. Brehelin, and J. A. Hoffmann.** 1974. Modifications of the hemogram and of the hemocytopoietic tissue of male adults of *Locusta migratoria* (Orthoptera) after injection of *Bacillus thuringiensis*. J. Invertebr. Pathol. **24:**238–247.

12. **Hoffmann, J. A.** 1970. The hemopoietic organs of the two orthopterans *Locusta migratoria* and *Gryllus bimaculatus*. Z. Zellforsch. Mikrosk. Anat. **106:**451–472.

13. **Howard, R. W., J. S. Miller, and D. W. Stanley.** 1998. The influence of bacterial species and intensity of infections on nodule formation in insects. J. Insect Physiol. **44:**157–164.

14. **Martens, E. C., K. Heungens, and H. Goodrich-Blair.** 2003. Early colonization events in the mutualistic association between *Steinernema carpocapsae* nematodes and *Xenorhabdus nematophila* bacteria. J. Bacteriol. **185:**3147–3154.

15. **Ouahrani-Bettache, S., F. Porte, J. Teyssier, J. P. Liautard, and S. Kohler.** 1999. pBBR1-GFP: a broad-host-range vector for prokaryotic promoter studies. BioTechniques **26:**620–622.

16. **Park, Y., and Y. Kim.** 2000. Eicosanoids rescue *Spodoptera exigua* infected with *Xenorhabdus nematophilus*, the symbiotic bacteria to the entomopathogenic nematode *Steinernema carpocapsae*. J. Insect Physiol. **46:**1469–1476.

17. **Park, Y., Y. Kim, S. M. Putnam, and D. W. Stanley.** 2003. The bacterium *Xenorhabdus nematophilus* depresses nodulation reactions to infection by inhibiting eicosanoid biosynthesis in tobacco hornworms, *Manduca sexta*. Arch. Insect Biochem. Physiol. **52:**71–80.

18. **Poinar, G. O., and P. T. Himsworth.** 1967. *Neoplectana* parasitism of larvae of the greater wax moth *Galleria mellonella*. J. Invertebr. Pathol. **9:**241–246.

19. **Poitout, S., and R. Bues.** 1970. Elevage de plusieurs espèces de lépidoptères Noctuidae sur milieu artificiel riche et sur milieu artificiel simplifié. Ann. Zool. Ecol. Anim. **2:**79–91.

20. **Renn, N.** 1998. Routes of penetration of the entomopathogenic nematode *Steinernema feltiae* attacking larval and adult houseflies (*Musca domestica*). J. Invertebr. Pathol. **72:**281–287.

21. **Ribeiro, C., B. Duvic, P. Oliveira, A. Givaudan, F. Palha, N. Simoes, and M. Brehélin.** 1999. Insect immunity—effects of factors produced by a nemato-bacterial complex on immunocompetent cells. J. Insect Physiol. **45:**677–685.

22. **Ribeiro, C., M. Vignes, and M. Brehélin.** 2003. *Xenorhabdus nematophila* (enterobacteriacea) secretes a cation-selective calcium-independent porin which causes vacuolation of the rough endoplasmic reticulum and cell lysis. J. Biol. Chem. **278:**3030–3039.

23. **Sicard, M., N. Le Brun, S. Pages, B. Godelle, N. Boemare, and C. Moulia.** 2003. Effect of native *Xenorhabdus* on the fitness of their *Steinernema* hosts: contrasting types of interaction. Parasitol. Res. **91:**520–524.

24. **Silva, C. P., N. R. Waterfield, P. J. Daborn, P. Dean, T. Chilver, C. P. Au, S. Sharma, U. Potter, S. E. Reynolds, and R. H. ffrench-Constant.** 2002. Bacterial infection of a model insect: *Photorhabdus luminescens* and *Manduca sexta*. Cell Microbiol. **4:**329–339.

25. **Thomas, G. M., and G. O. Poinar, Jr.** 1979. *Xenorhabdus* gen. nov., a genus of entomopathogenic nematophilic bacteria of the family *Enterobacteriaceae*. Int. J. Syst. Bacteriol. **29:**352–360.

26. **Vivas, E. I., and H. Goodrich-Blair.** 2001. *Xenorhabdus nematophilus* as a model for host-bacterium interactions: *rpoS* is necessary for mutualism with nematodes. J. Bacteriol. **183:**4687–4693.

27. **White, G.** 1927. A method for obtaining infective nematode larvae from culture. Science **66:**302–303.